Eur. Phys. J. C 26, 35–43 (2002)
Digital Object Identifier (DOI) 10.1007/s10052-002-1021-z

THE EUROPEAN PHYSICAL JOURNAL C

A simple model for nuclear structure functions at small x in the dipole picture

N. Armesto

Departamento de Física, Módulo C2, Planta baja, Campus de Rabanales, Universidad de Córdoba, 14071 Córdoba, Spain

Received: 5 June 2002 / Revised version: 27 June 2002 /
Published online: 16 October 2002 – © Springer-Verlag / Società Italiana di Fisica 2002

Abstract. A simple model for nuclear structure functions in the region of small x and small and moderate Q^2 is presented. It is a parameter-free extension, in the Glauber–Gribov approach to nuclear collisions, of a saturation model for the nucleon. A reasonable agreement with experimental data on the ratios of nuclear structure functions is obtained. Nuclear effects in the longitudinal-to-transverse cross section ratios are found to be small. Predictions of the model for values of x smaller than those available to present experiments are given. The unintegrated gluon distribution and the behaviour of the saturation scale which result from this model are shown and discussed.

1 Introduction

The differences between the structure functions measured in nucleons and nuclei [1], the so-called EMC effect, are a very important feature for the study of nuclear structure and nuclear collisions. At small values of the Bjorken variable x ($\lesssim 0.01$, shadowing region), the structure function F_2 per nucleon turns out to be smaller in nuclei than in a free nucleon. The nature of this shadowing is well understood qualitatively: In the rest frame of the nucleus, the incoming photon splits, at high enough Q^2, into a $q\bar{q}$ pair long before reaching the nucleus, and this $q\bar{q}$ pair interacts with it with typical hadronic cross sections, which results in absorption [2–6]; in this way nuclear shadowing is a consequence of multiple scattering and is thus related with diffraction [7]. An equivalent explanation in the frame in which the nucleus is moving fast, is that gluon recombination due to the overlap of the gluon clouds from different nucleons makes the gluon density in nucleus with mass number A smaller than A times that in a free nucleon [8, 9]. These studies have received a great theoretical impulse with the development of semiclassical ideas in QCD and the appearance of non-linear equations for the evolution in x in this framework [10–16], although saturation appears, different from shadowing [17] (see [18] for a simple geometrical approach in this framework).

On the other hand, a different approach is taken in [19]: the parton densities inside the nucleus are parameterised at some scale $Q_0^2 \sim 2\,\mathrm{GeV}^2$ and then evolved using the DGLAP [20] evolution equations. In this way, the origin of the differences of the parton densities in nucleons with respect to the nuclei is not addressed, but contained in the parameterisation at Q_0^2 which is obtained from a fit to the experimental data.

The results from different models usually depend on additional semiphenomenological assumptions and often contradict each other. For example, concerning the Q^2-dependence of the effect, in [3–5] it is argued that $q\bar{q}$ configurations of a large dimension give the dominant contribution to the absorption, with results essentially independent of Q^2 (this is the case in [6] until an extremely small x, where a dependence $\propto \ln Q/Q$ appears, related with the use of BFKL evolution [21]). On the other hand, in the gluon recombination approach of [9] the absorption is obtained as a clear higher-twist effect dying out at large Q^2. Finally, in the models [19] which use DGLAP, all Q^2-dependence comes from QCD evolution and is thus of a logarithmic, leading-twist nature; see [22] for a comparison between the multiple scattering and DGLAP approaches. Predictions (particularly for the gluon density) on the x-evolution towards small x turn out to be very different [23, 24].

In practice these studies are of the utmost importance to compute particle production in collisions involving nuclei. For example, in the framework of collinear factorization [25], parton densities in the nucleus following the spirit of [19] are needed; see e.g. [26] for recent applications to inclusive particle production in heavy ion collisions. While this scheme is suitable to compute particle production at scales $\Lambda^2_{\mathrm{QCD}} \ll Q^2 \lesssim s$ and thus in the hard region, for semihard (minijet) production, $\Lambda^2_{\mathrm{QCD}} \ll Q^2 \ll s$, the k_{T}-factorization scheme [27] should become the suitable one (in [28–30] applications to heavy ion collisions can be found). Here the tool that is needed is the so-called unintegrated gluon distribution (see for a precise definition below and [31] for a review for nucleons). Let us stress that different approaches give very different predictions for the multiplicities at RHIC and LHC [32].

In this paper we present a simple model for nuclear structure functions in the region of small x ($\lesssim 0.01$) and of small and moderate Q^2 ($\lesssim 20\,\mathrm{GeV}^2$) in the dipole pic-

ture [3,33]. It consists of an extension to nuclei, using the Glauber–Gribov picture [34], of the saturation model for the proton in [35] without any new parameter (in [30] a similar strategy is used but with a simplified dipole–nucleon cross section and no comparison with experimental data on nuclear structure functions is performed; also in [16] this ansatz is used but just as an initial condition for a non-linear evolution equation). The plan of this paper is as follows: In the next section the model will be described. In Sect. 3 a comparison of the results of the model with the available data on F_{2A} will be shown. In Sect. 4 the unintegrated gluon density obtained in this model, together with the saturation scale it implies, will be discussed. Finally, in the last section conclusions and possible applications of the model will be outlined.

2 Description of the model

The nuclear structure function F_2 can be standardly defined via the cross sections $\sigma_{\mathrm{T,L}}$ for the collision of the transversal (T) or longitudinal (L) virtual photon of momentum q, $q^2 = -Q^2$, on the nucleus A of momentum Ap:

$$F_{2A}(x,Q^2) = \frac{Q^2}{\pi e^2}(\sigma_{\mathrm{T}}^A + \sigma_{\mathrm{L}}^A); \tag{1}$$

this expression holds for the small x-region where we are going to work. Both cross sections can be conveniently presented in the dipole model [3,33] via the cross section $\sigma_{dA}(x,r)$, for the scattering of a colour dipole of transverse size r on the nucleus:

$$\sigma_{\mathrm{T,L}}^A(x) = \int \mathrm{d}^2 r \rho_{\mathrm{T,L}}(r)\sigma_{dA}(x,r), \tag{2}$$

where $\rho_{\mathrm{T,L}}$ are the distributions of colour dipoles created by splitting of the incident photon into $q\bar{q}$ pairs [3]:

$$\rho_{\mathrm{T}}(r) = \frac{e^2 N_c}{8\pi^3}\sum_f z_f^2 \int_0^1 \mathrm{d}\alpha \times \left\{[\alpha^2 + (1-\alpha)^2]\epsilon^2 K_1^2(\epsilon r) + m_f^2 K_0^2(\epsilon r)\right\} \tag{3}$$

and

$$\rho_{\mathrm{L}}(r) = \frac{e^2 N_c}{2\pi^3} Q^2 \sum_f z_f^2 \int_0^1 \mathrm{d}\alpha \alpha^2 (1-\alpha)^2 K_0^2(\epsilon r). \tag{4}$$

Here summation goes over flavours (which will be limited to 3 or 4, see the comments below (6)), $\epsilon^2 = Q^2\alpha(1-\alpha) + m_f^2$, and m_f and z_f are respectively the mass and electric charge in units of the proton charge e, of the quark of flavour f.

For the total cross section of a dipole on a proton we will use the saturation model in [35], which provides a good description of inclusive and diffractive experimental data on F_{2p} for $x < 0.01$ and small and moderate $Q^2 < 20\,\mathrm{GeV}^2$. Other models which also describe data in this region could be used, as that in [36]; see [37] for a comparison between this model and that of [35], which we will employ because of its simplicity. The form of the cross section is[1]

$$\sigma_{dp}(x,r) = \sigma_0\left[1 - \exp\left(-\frac{Q_{\mathrm{s}}^2(x) r^2}{4}\right)\right], \tag{5}$$

with

$$Q_{\mathrm{s}}^2(x) = Q_0^2\left(\frac{x_0}{\tilde{x}}\right)^\lambda, \quad \tilde{x} = x\left(1 + \frac{4m_f^2}{Q^2}\right). \tag{6}$$

In [35] some parameters were kept fixed: $Q_0^2 = 1\,\mathrm{GeV}^2$, $m_u = m_d = m_s = 0.14\,\mathrm{GeV}$ and $m_c = 1.5\,\mathrm{GeV}$. Three parameters were determined from a fit to the data and have values $\sigma_0 = 23.03$ (29.12) mb, $\lambda = 0.288$ (0.277) and $x_0 = 3.04 \cdot 10^{-4}$ ($0.41 \cdot 10^{-4}$) for the 3-flavour (4-flavour) version of the model. Q_{s}^2 is called the saturation scale, which we will discuss in Sect. 4.

Let us comment that, neglecting the influence of quark masses in the variable ϵ which has [38] a small effect in the case of light quarks, this model implies, in its 3-flavour version, an exact scaling of the cross sections $\sigma_{\mathrm{T,L}}^A$ with $\tau = Q^2/Q_{\mathrm{s}}^2$. This scaling has been shown [38] to be fulfilled to a good approximation by all DIS data for $x < 0.01$ (which go up to $Q^2 \sim 450\,\mathrm{GeV}^2$)[2]. So this model, which leads for large Q^2 to Bjorken scaling, is apparently able to mimic along a wide Q^2-region the QCD evolution (see [39] for improvements of this model to include DGLAP evolution). This τ-scaling has been argued to hold for such a large $Q^2 > Q_{\mathrm{s}}^2$ ($\sim 1\,\mathrm{GeV}^2$ in the region where data are available) in the framework of semiclassical, high-density QCD models [40], and has also been found in numerical solutions of the non-linear evolution equations at small x [13,15]. Let us also point out that this model does not correspond to any fixed twist; see [41] for a study of its twist structure.

The extension of this model to the nuclear case can be made in a straightforward manner in the Glauber–Gribov approach [34]: ignoring isospin effects which are negligible at small x where the model will be applied, we will substitute $\sigma_{dp}(x,r)$ by

$$\sigma_{dA}(x,r) = \int \mathrm{d}^2 b \sigma_{dA}(x,r,b), \tag{7}$$

with b the impact parameter of the center of the dipole relative to the center of the nucleus and

$$\sigma_{dA}(x,r,b) = 2\left[1 - \exp\left(-\frac{1}{2}AT_A(b)\sigma_{dp}(x,r)\right)\right] \tag{8}$$

[1] In this model no impact parameter of the proton is explicitly given, so it cannot be considered a pure eikonalization of some elementary amplitude [17]; on the contrary, in our extension to nuclei, (7) and (8) below, the impact parameter of the nucleus is explicitly taken into account

[2] In the 4-flavour version, a flavour dependence is introduced in Q_{s}^2 through the variable $\tilde{x}$ and some deviation of the scaling may also appear through the variable ϵ in the photon wave function due to the larger charm mass

the total dipole–nucleus cross section for fixed impact parameter, with $\sigma_{dp}(x,r)$ given by (5) and (6). $T_A(b)$ is the nuclear profile function (longitudinal integral of the nuclear density, $T_A(b) = \int_{-\infty}^{\infty} \mathrm{d}z \rho_A(z,\vec{b})$) normalized to unity, $\int \mathrm{d}^2 b T_A(b) = 1$; we employ a nuclear density in the form of a 3-parameter Fermi distribution with parameters taken from [42]. With this normalization we recover the dipole–nucleon cross section making a power expansion for small $AT_A(b)\sigma_0$, keeping the first term and putting $A = 1$. Also the centrality (impact parameter) dependence of the structure functions can be computed by direct substitution of $\sigma_{dA}(x,r,b)$, (8), into (2). This model implies a new scaling for nucleus of the type of the τ-scaling for proton and a new saturation scale, which we will discuss in Sect. 4. These two equations, (7) and (8), constitute the central point in our extension of the model of [35] to the nuclear case.

Using (1)–(8) we can compute the nucleon and nuclear structure functions and the corresponding ratios, which we will compare with the experimental data in the next section. But first let us discuss the region of applicability of the model: This should be that of small x (due to the use of the model of [35] for the nucleon, to the neglect of isospin effects and to the use of (8) which requires a large coherence length, achieved at small x, of the photon fluctuation), and of small and moderate values $Q^2 < 20\,\mathrm{GeV}^2$. Although the τ-scaling may suggest that the region of applicability in Q^2 could be wider, we think that a safe extrapolation to higher Q^2 would require one to implement DGLAP evolution [39]. Also the extrapolation to very small x could imply effects of gluon or pomeron fusion like those included in the non-linear evolution equations mentioned previously, so it should be taken with care. Nevertheless, numerical studies [15] show that the onset of the non-linear effects is quite smooth, becoming large for extremely small x. So we consider[3] this model as a reasonable approximation for values of $x \gtrsim 10^{-5} \div 10^{-6}$, which are those relevant for RHIC and LHC. Due to the fact that for nuclear structure functions the amount of experimental data is much more limited than that for nucleons, we will perform the comparison with experimental data for $x < 0.02$.

3 Comparison with experimental data

Here we show the results of the model together with available experimental data. In Figs. 1–5, the results of the model in the 3-flavour (solid lines) and 4-flavour (dashed lines) versions (see the explanations below (6)) are compared with the experimental data from [43–46]. In these figures $R(A/B) = [BF_{2A}(x,Q^2)]/[AF_{2B}(x,Q^2)]$. Even when joined with a line, the results of the model have been computed at the same $(\langle x\rangle, \langle Q^2\rangle)$ as the experimental data; in the latter, the inner error bars are the statistical errors, while the outer error bars show statistical and systematic errors added in quadrature (with overall normalization uncertainties ignored). Considering both the absence of any free parameter in going from the nucleon to the nuclear case and the simplicity of the model, we find the agreement quite reasonable. Concretely, from Figs. 3 and 4 it can be concluded that the A- and Q^2-dependences

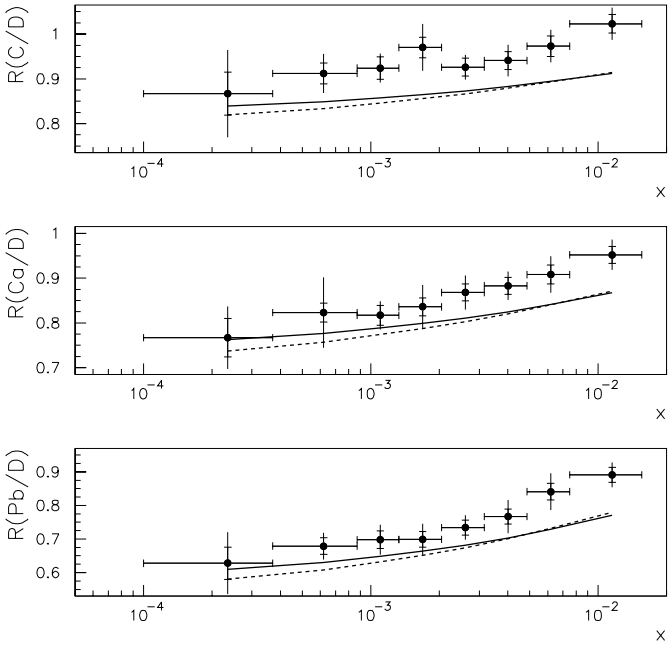

Fig. 1. Comparison of the results of the model (see text) in the 3-flavour (solid lines) and 4-flavour (dashed lines) versions with experimental data at small x for the ratios C, Ca and Pb over D, from [43]

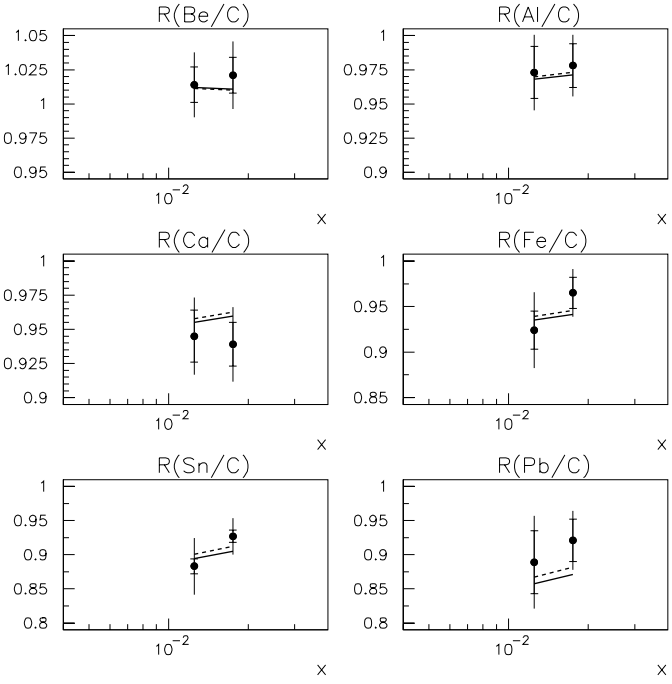

Fig. 2. Same as Fig. 1 but with data for Be, Al, Ca, Fe, Sn and Pb over C, from [44]

[3] In [15] it is seen that the scaling induced by the non-linear evolution is fulfilled for values of $y = [\pi/(N_c\alpha_s)]\ln(x_0/x)$ greater than 2.2, which for $\alpha_s = 0.2$ and $x_0 = 0.01$ means x smaller than 10^{-7}

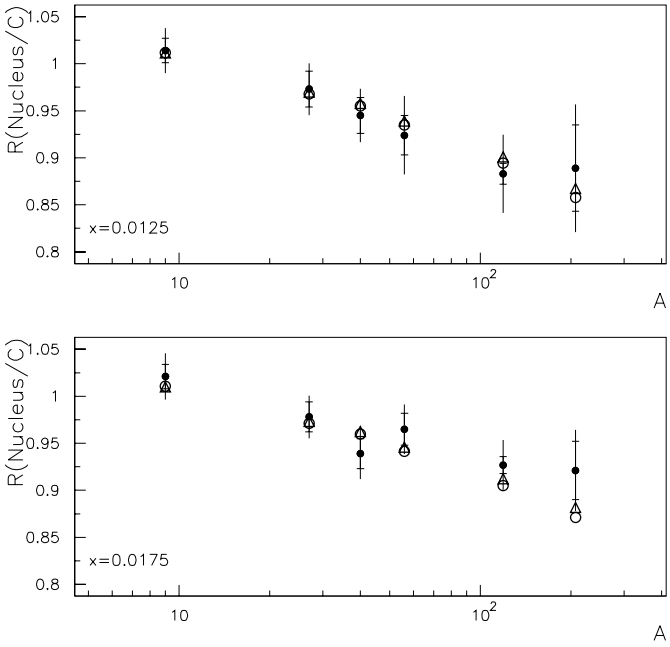

Fig. 3. Comparison of the A-evolution of the results of the model in the 3-flavour (open circles) and 4-flavour (open triangles) versions with experimental data at small fixed x for Be, Al, Ca, Fe, Sn and Pb over C, from [44]

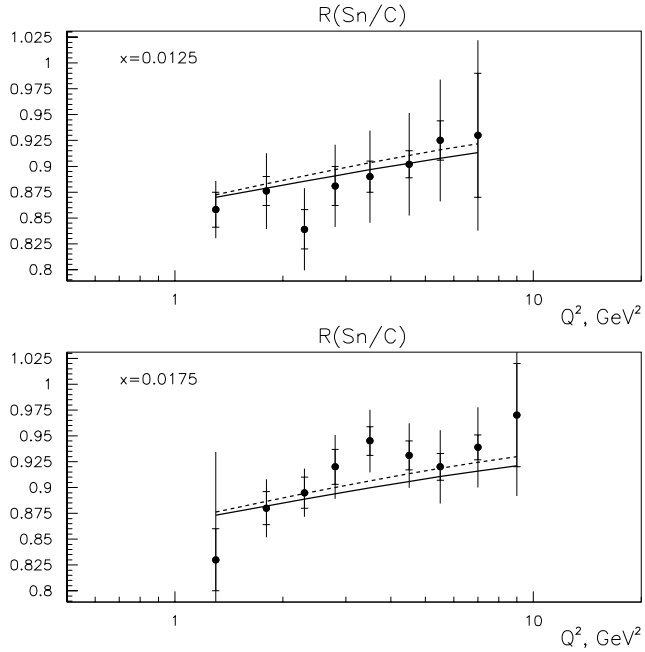

Fig. 4. Comparison of the Q^2-evolution of the model in the 3-flavour (solid lines) and 4-flavour (dashed lines) versions with experimental data for Sn over C at small fixed x, from [45]

of the data at fixed x are well reproduced, while in Figs. 1, 2 and 5 the x-dependence is reasonably reproduced, taking into account that these latter figures contain data with Q^2 going from $\sim 0.15\,\mathrm{GeV}^2$ for the smallest x values to $\sim 4.5\,\mathrm{GeV}^2$ for the highest x.

As the version with three flavours is simpler, gives an equally reasonable agreement with nuclear data than the 4-flavour version, and produces a better description of the nucleon data [35], from now on we will restrict our computations to the 3-flavour version.

Let us turn now to the behaviour of the ratio of longitudinal to transverse cross sections. Experimentally [47] large nuclear effects have been observed: the ratio $\sigma_{\mathrm{L}}/\sigma_{\mathrm{T}}$ in N (^{3}He) over $\sigma_{\mathrm{L}}/\sigma_{\mathrm{T}}$ in D has been found to reach values as high as ~ 5 (~ 2) for $0.01 < x < 0.03$ and $Q^2 < 1\,\mathrm{GeV}^2$. Some explanations [48] point to nuclear enhanced power corrections, but the experimental data are under reanalysis [49] and the evidence of such strong nuclear effects is now dubious. While this important point has to be settled, it is clear than in our model such strong effects are not present, as the nuclear effects are contained in the Glauber–Gribov cross section in (7) and (8) which is common to both longitudinal and transverse cross sections; see (2). In Fig. 6 we show the results in our model for the ratio $\sigma_{\mathrm{L}}/\sigma_{\mathrm{T}}$ in the nucleus over $\sigma_{\mathrm{L}}/\sigma_{\mathrm{T}}$ in the proton, for C and Pb. It can be seen that the nuclear effects never go beyond $\pm 12\%$, which is a clear prediction of our model.

In Fig. 7 we present predictions of the model for the ratio $F_{2A}/(AF_{2p})$ for C and Pb, together with the x-evolution for Be, C, Al, Ca, Fe, Sn and Pb at fixed $Q^2 = 2.25\,\mathrm{GeV}^2$. A clear evolution with Q^2 can be seen, which in this model is due to the interplay between the (transversal and longitudinal) probabilities to get a dipole of size r;

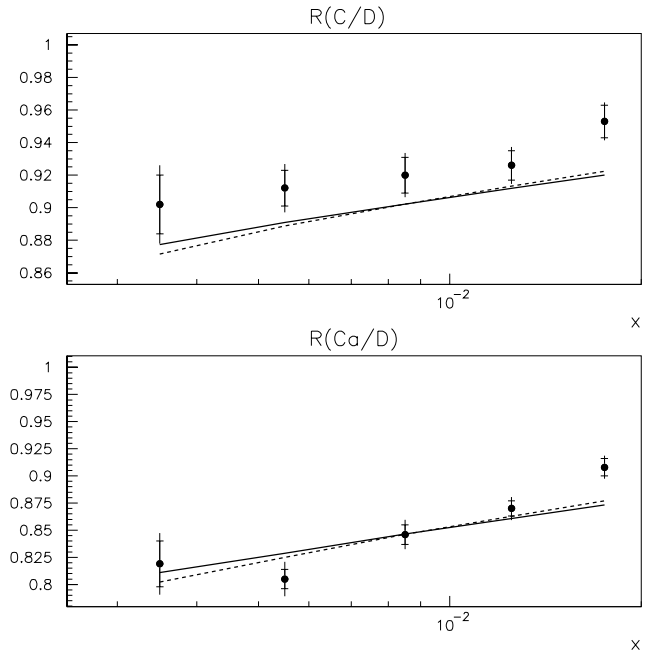

Fig. 5. Same as Fig. 1 but with data for C and Ca over D, from [46]

see (3) and (4), and the dipole-target cross section; see (5), (7) and (8), and cannot be addressed to any concrete twist but to an admixture of all twists [41]. At large enough Q^2 this dependence on Q^2 will eventually disappear, as this model, as stated previously, leads to Bjorken scaling.

As a last point in this section, let us comment on other possible options to get nuclear structure functions in the framework of the dipole model. A simple form for the

dipole–nucleus cross section is suggested by high-density QCD [10,12,17]:

$$\sigma_{dA}(x,r) = \int \mathrm{d}^2 b \left[1 - \exp\left(-\frac{Q_{\mathrm{s}A}^2(b) r^2}{4}\right)\right]. \quad (9)$$

We have tried several relations between $Q_{\mathrm{s}A}^2$ (the saturation scale in nuclei) and that in the proton, Q_s^2. On the one hand, we have used a relation coming from the running of the coupling, of the type

$$Q_{\mathrm{s}A}^2 \ln\left(\frac{Q_{\mathrm{s}A}^2}{\Lambda_{\mathrm{QCD}}^2}\right) \propto \left(\frac{T_A(b)}{T_A(0)}\right) A^{1/3} Q_s^2 \ln\left(\frac{Q_s^2}{\Lambda_{\mathrm{QCD}}^2}\right). \quad (10)$$

On the other hand, we have imposed the first scattering approximation (valid for $r \to 0$) in (8),

$$Q_{\mathrm{s}A}^2 = \frac{1}{2} A T_A(b) \sigma_0 Q_s^2 \quad (11)$$

(in this expression the value of the running coupling evaluated at the appropriate scale is hidden in σ_0, see e.g. [17])[4]. But so far we have not succeeded in getting a satisfactory description of the experimental data, not even on a qualitative level: either too strong a shadowing is observed or too fast an evolution in x (and too slow in Q^2) is obtained. Indeed (8) and (9) contain different physical assumptions on the nature of the scattering centers: while (8) considers multiple scattering on single nucleons (described by the saturating form (5)), (9) implies scattering on a black area filled with partons coming from many nucleons. Our lack of success in reproducing the experimental data with (9) suggests that higher order rescatterings are actually needed in the exponent of (5) for the proton, and that the asymptotic region where (9) should be valid to describe data on F_{2A} integrated over the impact parameter, is not reached yet (i.e. the grey region is still dominating the scattering); a very important test for the form (9) would be its ability to describe the experimental data on diffraction (which is indeed fulfilled by (5) [35]). In the next section we will address the behaviour of the saturation scale in our model.

4 Unintegrated gluon distribution and saturation scale

As stated in the Introduction, in the k_{T}-factorization scheme [27] a key ingredient is the unintegrated gluon distribution of the hadron, $\varphi_A(x,k,b)$ (sometimes it appears

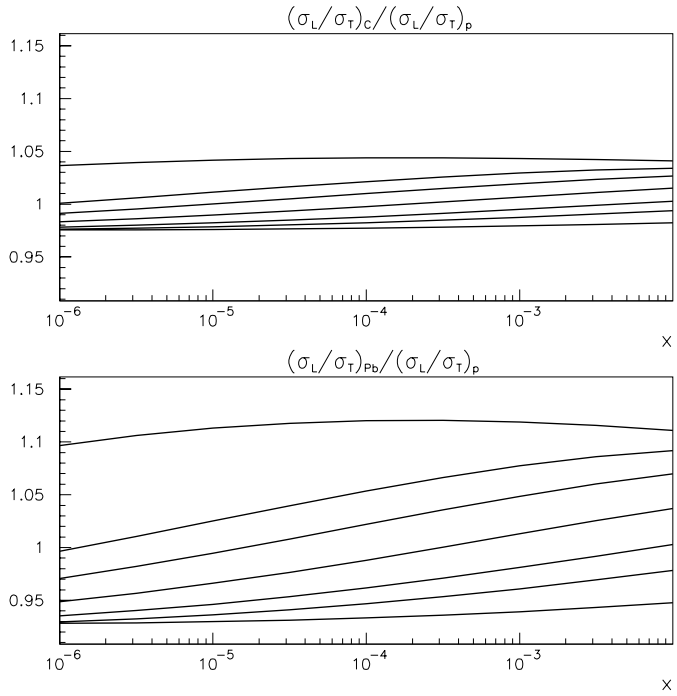

Fig. 6. Results of the model for the ratio $\sigma_{\mathrm{L}}/\sigma_{\mathrm{T}}$ in C and Pb over $\sigma_{\mathrm{L}}/\sigma_{\mathrm{T}}$ in proton versus x. In the plots, lines going from the bottom to the top correspond to $Q^2 = 0.1$, 0.5, 1, 2.25, 5, 10 and 100 GeV^2

in the literature as $f = k^2\varphi$ [28,31]), with k the transverse momentum. This $\varphi_A(x,k,b)$ at fixed impact parameter b is related, at lowest order in k_{T}-factorization [31], to the dipole–nucleus cross section by a Bessel–Fourier transform (see [15,16]):

$$\varphi_A(x,k,b) = -\frac{N_c}{4\pi^2\alpha_{\mathrm{s}}} k^2 \int \frac{\mathrm{d}^2 r}{2\pi} \exp\left(\mathrm{i}\vec{k}\cdot\vec{r}\right) \sigma_{dA}(x,r,b), \quad (12)$$

with $k^2 = \vec{k}\cdot\vec{k}$, $r^2 = \vec{r}\cdot\vec{r}$ and vectors defined in the two-dimensional transverse space. The unintegrated gluon can be related to the "ordinary" gluon density (that used in collinear factorization [25]) by

$$xG(x,Q^2,b) = \int^{Q^2} \mathrm{d}k^2 \varphi_A(x,k,b), \quad (13)$$

although this expression must be considered with great care, as it is only true for large $Q^2 \gg Q_{\mathrm{s}}^2$ (the actual relation is not with the collinear glue but with the gluon distribution in the light-cone wave function of the hadron; see [10,12,17]).

For the proton, (12) leads to the result $\varphi_p(x,k) \propto \sigma_0 (k^2/Q_{\mathrm{s}}^2) \exp\left(-k^2/Q_{\mathrm{s}}^2\right)$ [35][5]. For the nucleus, using the technique outlined in the appendix of [16] (or simply applying $[N_c/(2\pi^2\alpha_{\mathrm{s}})] k^2 \nabla_k^2$ to the function ϕ_0 defined in (31) and (34) in that reference), we get

[4] The fact that $Q_{\mathrm{s}A}^2$ and Q_s^2 may have roughly the same x-dependence can be justified by the following qualitative argument: $Q_{\mathrm{s}A}^2$ is related with p_{T}-broadening in the nucleus, $Q_{\mathrm{s}A}^2 = n_A(b) Q_s^2$, with $n_A(b)$ the number of scatterings at impact parameter b. As $n_A(b) \propto A T_A(b) x G \alpha_{\mathrm{s}}(Q_{\mathrm{s}A}^2)/Q_{\mathrm{s}A}^2$ (for a perturbative QCD cross section evaluated at scale $Q_{\mathrm{s}A}^2$ and xG the gluon distribution in a nucleon) and $Q_s^2 \propto xG$, $Q_{\mathrm{s}A}^2$ and Q_s^2 show the same x-behaviour (modulo the logarithm coming from the running coupling). Special thanks are given to D.E. Kharzeev for discussions and suggestions on all these points

[5] In some proposals [12,29] it is considered that the unintegrated gluon distribution should tend to a constant as $k \to 0$. For discussions on the "correct" definition and behaviour of this quantity, see [15,30]

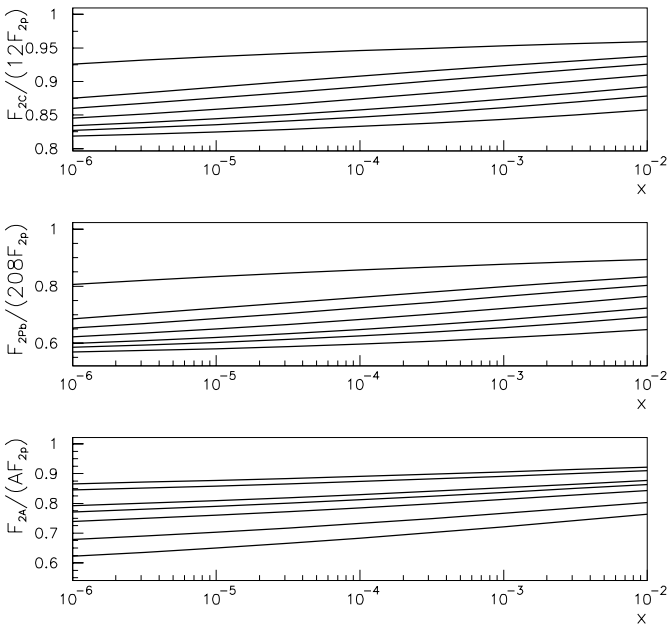

Fig. 7. Results of the model for the x-dependence of $F_{2A}/(AF_{2p})$. In the two upper plots, results for C (upper plot) and Pb (plot at the middle) versus x are given for $Q^2 = 0.1$, 0.5, 1, 2.25, 5, 10 and 100 GeV^2 (lines going from the bottom to the top). In the plot at the bottom, $F_{2A}/(AF_{2p})$ is drawn versus x at $Q^2 = 2.25\,\mathrm{GeV}^2$ for Be, C, Al, Ca, Fe, Sn and Pb (lines going from the top to the bottom)

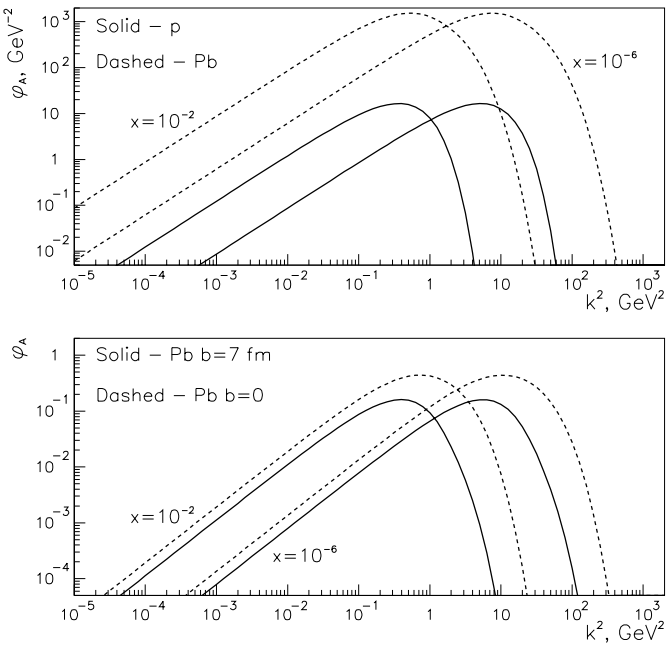

Fig. 8. Upper plot: Results of the model (in GeV^{-2}) for the unintegrated gluon distribution for proton (solid line) and for Pb integrated over b (dashed line). Lower plot: Results of the model for the unintegrated gluon distribution for peripheral ($b = 7\,\mathrm{fm}$, solid line) and central ($b = 0$, dashed line) Pb. In each case, two curves are provided for two values of $x = 10^{-2}$ (curve to the left) and 10^{-6} (curve to the right)

$$\varphi_A(x,k,b) = \frac{N_c}{\pi^2\alpha_s}\frac{k^2}{Q_s^2}\sum_{n=1}^{\infty}\frac{(-B)^n}{n!} \times \sum_{l=0}^{n} C_n^l \frac{(-1)^l}{l}\exp\left(-\frac{k^2}{lQ_s^2}\right), \qquad (14)$$

with

$$B = \frac{1}{2}AT_A(b)\sigma_0. \qquad (15)$$

As in the case of the proton, (14) shows explicit scaling in k^2/Q_s^2; besides, in this equation (as in (8)) the result for the proton is recovered making a power expansion for small B, keeping the first term and putting there $A = 1$. For realistic values of $B < 3$, (14) turns out to be very suitable for numerical computations, as the convergence of the series in n is very fast and only a few terms are needed to get $\varphi_A(x,k,b)$ to the desired accuracy.

In Fig. 8 we show the unintegrated gluon distribution for the proton, and for Pb in three cases: central ($b = 0$), peripheral ($b = 7\,\mathrm{fm}$), and integrated over b, and for two values of $x = 10^{-2}$ and 10^{-6} (in these computations there is no Q^2, so the substitution in (6) is meaningless here and we will make no distinction in this section between x and $\tilde{x}$; this also avoids the complication of flavour dependence in case the 4-flavour version is to be used, although as stated previously we will use the 3-flavour version). A scaling in k^2/Q_{sA}^2 (with Q_{sA}^2 identified with the position of the maximum; see below) is perfectly visible, as in each case the curves move to the right with decreasing x while keeping their shape and size (this phenomenon has also been found in the framework of the non-linear equations for small x [10,12,13,15] and the solution called a soliton wave [15]). Besides it can be seen that the shape of the curves for different cases is quite close, the only differences being the height, the position of the maximum which at fixed x varies from left to right for proton and Pb with increasing centrality, and the logarithmic width which slightly increases with increasing centrality (being e.g. at 1/10 of the maximum height, 2.20 for the proton and 2.40 for central Pb).

Keeping in mind the difficulties to identify at small and moderate Q^2 the integral of the unintegrated gluon distribution with the ordinary gluon density, (13) (see the comments below it), it is still tempting to use this equation and compare with other approaches. A comparison at $Q^2 = 5\,\mathrm{GeV}^2$ of the results of our model with others, for the ratio of gluon densities in Pb over proton, can be found in [24]. There it can be seen that our results at $x \simeq 10^{-2}$ roughly coincide with those of [19,50] and are higher than those of [22,51], while at $x \simeq 10^{-5}$ they become smaller than those of [19,50], get close to those of [22] and are still larger than those of [51]. Apart from the constraints coming from the existing DIS experimental data on nuclei which are very loose for the glue at small x, in [19] the saturation of gluon shadowing comes mainly from the initial condition for the DGLAP evolution where this saturation has been imposed, while [22, 50] are theoretical models and in [51] the behaviour of the glue has been fixed in order to reproduce charged particle multiplicities in AuAu collisions at RHIC. Additional

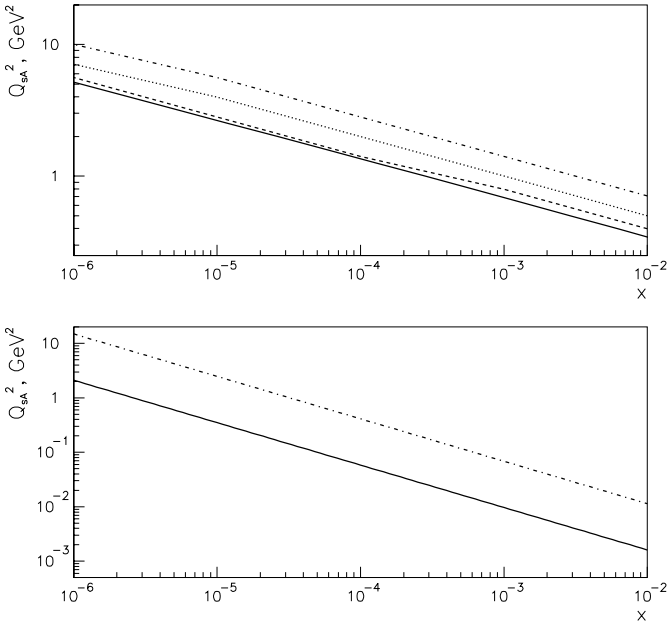

Fig. 9. Upper plot: saturation momentum in the model for proton (solid line), and for Pb in three cases: central ($b = 0$, dashed-dotted line), peripheral ($b = 7$ fm, dashed line), and integrated over b (dotted line). Lower plot: saturation momentum in the numerical solution of the non-linear equation in [15], (17), for $A = 1$ (solid line) and $A = 208$ (dashed-dotted line). Notice the difference in vertical scales between the plots

caution has to be taken to compare our results with those coming from DGLAP analysis [19]: our ratios for the glue at some moderate, fixed Q^2 and very small x are found to result with values smaller than the ratios for F_2 at the same x, Q^2, which leads to problems with leading-twist DGLAP evolution [23]; as our model mimics the DGLAP increase of F_2 along a wide Q^2-region, this is most probably related with the use of (13) at too small Q^2. In any case, our model leads to Bjorken scaling at some Q^2 which increases with decreasing x: the Q^2-independence of the gluon density is achieved in our model at $Q^2 \simeq 15\,\mathrm{GeV}^2$ for $x = 10^{-2}$ and at $Q^2 \simeq 300\,\mathrm{GeV}^2$ for $x = 10^{-6}$. Of course this is due to the exponential decrease of the unintegrated gluon at large k^2; see (14). Other proposals (see e.g. [12,29]) consider a behaviour $\propto 1/k^2$ at large k^2 which obviously leads to a logarithmic, DGLAP-like increase of the gluon density with increasing Q^2.

Now we turn to the saturation scale. While for the case of the proton its definition is quite clear in coordinate space, for the nucleus a clean definition is better obtained in momentum space, where it corresponds to the maximum of the unintegrated gluon distribution [12,13, 15,52]. The results are shown in Fig. 9 (upper plot) for the same cases as in Fig. 8. Contrary to naive expectations, the saturation scale between proton and central nucleus is not simply proportional to $A^{1/3}$ but has a prefactor which makes the result smaller (turning the expected factor 5.9 for Pb into a factor 2.0). This can be understood using analytical estimates. Taking the exponent in (8) to be 1/4 (in analogy to the case of the proton), we get

$$Q_{sA}^2 \simeq \left[4\ln\left(\frac{2AT_A(b)\sigma_0}{2AT_A(b)\sigma_0 - 1}\right)\right]^{-1} Q_s^2, \qquad (16)$$

which gives a $Q_{sA}^2 \simeq 2.4 Q_s^2$ for Pb at $b = 0$. For $AT_A(b)\sigma_0 \gg 1$, we get exactly (11), recover the expected proportionality $Q_{sA}^2 \propto A^{1/3} Q_s^2$ and find with this asymptotic form $Q_{sA}^2 \simeq 2.5 Q_s^2$. As the form (8) gives a nice agreement with the data and (9) and (11) do not, we conclude that preasymptotic contributions (i.e. not corresponding to $AT_A(b)\sigma_0 \to \infty$) play a dominant role for the description of the presently available data.

To perform some comparison with other approaches, let us see the saturation scale coming from the numerical solution of the non-linear evolution equation in [15]. There a form (for the evolution obtained starting from a phenomenologically motivated initial distribution) is obtained that can be approximated, for central ($b = 0$) Pb, by the equation

$$Q_{sA}^2 \simeq A^{0.37} \exp\left[-6.43 + 0.78 \ln\left(\frac{x_0}{x}\right)\right]; \qquad (17)$$

here $x_0 = 0.01$, the value of $\alpha_s = 0.2$ has been used and the result is in GeV^2. The coefficients in this equation coincide with those obtained in other numerical and analytical studies [12,13,40]. Its results for $A = 1$ and $A = 208$ are shown in Fig. 9 (lower plot), but one should keep in mind the way in which the coefficients in (17) were obtained [15]: They come from a fit to the position of the maximum of the unintegrated gluon distributions for different centralities and values of x but when the scaling induced by the non-linear evolution has already set in. So, from the first footnote it can be concluded that they correspond to $x < 10^{-7}$ and thus to a much lower value of x than the region where we have actually plotted them in Fig. 9. From the comparison of the two plots in Fig. 9 it is clear that the non-linear evolution produces a much steeper behaviour compared with the model in this paper (i.e. an exponent 0.78 compared to 0.288), while the asymptotic A-dependence is not really different ($0.37 \simeq 1/3$).

5 Conclusions

A simple model for nuclear structure functions in the region of small x, and small and moderate Q^2, has been presented. It is a parameter-free extension of the saturation model for the nucleon of [35] in the Glauber–Gribov approach, although in principle any saturating model which correctly describes the nucleon data, e.g. [36], could be used. This simple extension of the model for the nucleus should be valid until non-linear evolution effects [10–16] become of importance, and for not too high Q^2 where the implementation of the DGLAP evolution should be required. Conservative estimates establish the region of validity of the model to be $10^{-5} \div 10^{-6} < x < 10^{-2}$ and $Q^2 < 20\,\mathrm{GeV}^2$.

A reasonable agreement with the experimental data is obtained for the x-, A- and Q^2-dependence. The longitudinal-to-transverse cross section ratios show nuclear effects

smaller than ±12%. Predictions of the model for values of x smaller than those available to present experiments have been given.

The unintegrated gluon distribution coming from our dipole–nucleus cross section has been obtained and studied. Besides this, the behaviour of the saturation scale in this model has been shown and discussed. It turns out to behave $\propto A^{1/3}$ for large A, as expected, but large prefactors make the resulting scale for the nuclei smaller than naive estimates, e.g. for central Pb 2 times bigger, instead of 6 times, than the corresponding scale for the proton.

Our model could be used to provide the starting condition for DGLAP evolution, as performed in the approaches of [19], for some initial scale $Q_0^2 \gg \Lambda^2_{\rm QCD}$. The unintegrated gluon distribution could be employed to compute the particle production, using the $k_{\rm T}$-factorization scheme [27,31], in high energy collisions involving nuclei [28–30]. Work along these directions is in progress.

A last comment: our study implies the existence of a scaling for nuclei of the same type as that for the proton [38], with a non-trivial relation for the A-dependence of the saturation scales between both cases, while the x-dependence turns out to be the same. An experimental, model-independent extraction of the saturation scale in nuclei would be very useful to settle the discussions on the relevance of the semiclassical approach for existing or future experiments, and the region of validity of the perturbative QCD and DGLAP evolution. Such an issue would be best explored, and our model tested, in high energy lepton–nucleus colliders [53].

Acknowledgements. The author expresses his gratitude to M.A. Braun, R. Engel, K. Itakura, V.J. Kolhinen, L. McLerran, C. Pajares, P.V. Ruuskanen, R. Venugopalan and U.A. Wiedemann, for useful discussions. Special thanks are given to K.J. Eskola and D.E. Kharzeev for their interest, suggestions and encouragement to write this article, and to A. Capella, E.G. Ferreiro and C.A. Salgado for discussions, suggestions and a critical reading of the manuscript. He also thanks CERN Theory Division, Departamento de Física de Partículas at Universidade de Santiago de Compostela, Department of Physics at University of Jyväskylä, Helsinki Institute of Physics and Physics Department at BNL, for kind hospitality during stays in which parts of this work have been developed. Finally he acknowledges financial support by CICYT of Spain under contract AEN99-0589-C02 and by Universidad de Córdoba.

References

1. M. Arneodo, Phys. Rep. **240**, 301 (1994); D.F. Geesaman, K. Saito, A.W. Thomas, Ann. Rev. Nucl. Part. Sci. **45**, 337 (1995)
2. S.J. Brodsky, T.E. Close, J.F. Gunion, Phys. Rev. D **6**, 177 (1972); S.J. Brodsky, H.J. Liu, Phys. Rev. Lett. **64**, 1342 (1990)
3. N.N. Nikolaev, B.G. Zakharov, Z. Phys. C **49**, 607 (1991)
4. V. Barone, M. Genovese, N.N. Nikolaev, E. Predazzi, B.G. Zakharov, Z. Phys. C **58**, 541 (1993)
5. B.Z. Kopeliovich, B. Povh, Phys. Lett. B **367**, 329 (1996)
6. N. Armesto, M.A. Braun, Z. Phys. C **76**, 81 (1997)
7. A. Capella, A.B. Kaidalov, C. Merino, D. Pertermann, J. Tran Thanh Van, Eur. Phys. J. C **5**, 111 (1998)
8. L.V. Gribov, E.M. Levin, M.G. Ryskin, Phys. Rept. **100**, 1 (1983)
9. A.H. Mueller, J.-W. Qiu, Nucl. Phys. B **268**, 427 (1986); J.-W. Qiu, Nucl. Phys. B **291**, 746 (1987); E.L. Berger, J.-W. Qiu, Phys. Lett. B **206**, 42 (1988)
10. L. McLerran, R. Venugopalan, Phys. Rev. D **49**, 2233, 3352 (1994); D **50**, 2225 (1994); J. Jalilian-Marian, A. Kovner, L. McLerran, H. Weigert, Phys. Rev. D **55**, 5414 (1997); E. Iancu, A. Leonidov, L. McLerran, Nucl. Phys. A **692**, 583 (2001); E. Iancu, L. McLerran, Phys. Lett. B **510**, 145 (2001); E.G. Ferreiro, E. Iancu, A. Leonidov, L. McLerran, Nucl. Phys. A **703**, 489 (2002); A. Kovner, U.A. Wiedemann, hep-ph/0112140; preprint CERN-TH-2002-089 (hep-ph/0204277); E.G. Ferreiro, E. Iancu, K. Itakura, L. McLerran, preprint SACLAY-T02/074, NSF-ITP-02-44 (hep-ph/0206241)
11. I.I. Balitsky, preprint JLAB-THY-97-22 (hep-ph/9706411); Nucl. Phys. B **463**, 99 (1996)
12. A.H. Mueller, Nucl. Phys. B **335**, 115 (1990); B **558**, 285 (1999); Yu.V. Kovchegov, A.H. Mueller, Nucl. Phys. B **529**, 451 (1998); Yu.V. Kovchegov, Phys. Rev. D **54**, 5463 (1996); D **55**, 5445 (1997)
13. E.M. Levin, K. Tuchin, Nucl. Phys. B **573**, 383 (2000); E.M. Levin, M. Lublinsky, Nucl. Phys. A **696**, 833 (2001); M. Lublinsky, Eur. Phys. J. C **21**, 513 (2001); K. Golec-Biernat, L. Motyka, A.M. Staśto, Phys. Rev. D **65**, 074037 (2002)
14. E. Gotsman, E.M. Levin, U. Maor, E. Naftali, Nucl. Phys. B **539**, 535 (1999); E.M. Levin, U. Maor, preprint TAUP-2643-2000 (hep-ph/0009217); A.L. Ayala, M.B. Gay Ducati, E.M. Levin, Nucl. Phys. B **493**, 305 (1997); M.B. Gay Ducati, V.P. Gonçalves, Phys. Lett. B **466**, 375 (1999)
15. M.A. Braun, Eur. Phys. J. C **16**, 337 (2000); hep-ph/0010041; N. Armesto, M.A. Braun, Eur. Phys. J. C **20**, 517 (2001)
16. N. Armesto, M.A. Braun, Eur. Phys. J. C **22**, 351 (2001)
17. A.H. Mueller, in Proceedings of the XVII Autumn School: QCD: Perturbative or Nonperturbative?, edited by L.S. Ferreira, P. Nogueira, J.I. Silva-Marcos (World Scientific, Singapore 2001), p. 180
18. N. Armesto, C.A. Salgado, Phys. Lett. B **520**, 124 (2001)
19. K.J. Eskola, V.J. Kolhinen, P.V. Ruuskanen, Nucl. Phys. B **535**, 351 (1998); K.J. Eskola, V.J. Kolhinen, C.A. Salgado, Eur. Phys. J. C **9**, 61 (1999); D. Indumathi, W. Zhu, Z. Phys. C **74**, 119 (1997); M. Hirai, S. Kumano, M. Miyama, Phys. Rev. D **64**, 034003 (2001)
20. Yu.L. Dokshitzer, Sov. Phys. JETP **46**, 1649 (1977); V.N. Gribov, L.N. Lipatov, Sov. J. Nucl. Phys. **15**, 438 (1972); G. Altarelli, G. Parisi, Nucl. Phys. B **126**, 298 (1977)
21. V.S. Fadin, E.A. Kuraev, L.N. Lipatov, Phys. Lett. B **60**, 50 (1975); I.I. Balitsky, L.N. Lipatov, Sov. J. Nucl. Phys. **15**, 438 (1978)
22. L. Frankfurt, V. Guzey, M. McDermott, M. Strikman, JHEP **0202**, 027 (2002)
23. K.J. Eskola, H. Honkanen, V.J. Kolhinen, C.A. Salgado, Phys. Lett. B **532**, 222 (2002); in Proceedings of the XXXVIIth Rencontres de Moriond: QCD and Hadronic Interactions, Les Arcs, France, March 16–23, 2002 (hep-ph/0205231)

24. C.A. Salgado, talk given at the Second Meeting of the CERN Workshop on Hard Probes in Heavy Ion Collisions at the LHC, Geneve, Switzerland, March 11–15, 2002 (http://wwwth.cern.ch/lhcworkshop/plenary_mar.html)
25. J.C. Collins, D.E. Soper, G. Sterman, Nucl. Phys. B **261**, 104 (1985); B **308**, 833 (1988); in Perturbative QCD, edited by A.H. Mueller (World Scientific, Singapore 1989), p. 1
26. K.J. Eskola, H. Honkanen, preprint HIP-2002-23/TH (hep-ph/0205048); K.J. Eskola, K. Kajantie, P.V. Ruuskanen, K. Tuominen, Nucl. Phys. B **570**, 379 (2000); preprint HIP-2002-10-TH, NORDITA-2002-20-HE (hep-ph/0204034)
27. S. Catani, M. Ciafaloni, F. Hautmann, Nucl. Phys. B **366**, 135 (1991); J.C. Collins, R.K. Ellis, Nucl. Phys. B **360**, 3 (1991); E.M. Levin.M.G. Ryskin, Yu.M. Shabelski, A.G. Shuvaev, Sov. J. Nucl. Phys. **53**, 657 (1991)
28. K.J. Eskola, A.V. Leonidov, P.V. Ruuskanen, Nucl. Phys. B **481**, 704 (1996); M. Gyulassy, L. McLerran, Phys. Rev. C **56**, 2219 (1997)
29. D.E. Kharzeev, M. Nardi, Phys. Lett. B **507**, 121 (2001); D.E. Kharzeev, E.M. Levin, Phys. Lett. B **523**, 79 (2001); D.E. Kharzeev, E.M. Levin, M. Nardi, preprint BNL-NT-01/28 (hep-ph/0111315)
30. H.-J. Pirner, F. Yuan, Phys. Lett. B **512**, 297 (2001)
31. B. Andersson et al., preprint DESY 02-041 (hep-ph/0204115)
32. N. Armesto, C. Pajares, Int. J. Mod. Phys. A **15**, 2019 (2000)
33. A.H. Mueller, Nucl. Phys. B **415**, 373 (1994); A.H. Mueller, B. Patel, Nucl. Phys. B **425**, 471 (1994)
34. R.J. Glauber, in Lectures in Theoretical Physics, Vol. 1, edited by W.E. Brittin, L.G. Duham (Interscience, New York 1959); V.N. Gribov, Sov. Phys. JETP **29**, 483 (1969); **30**, 709 (1970)
35. K. Golec-Biernat, M. Wüsthoff, Phys. Rev. D **59**, 014017 (1999); D **60**, 114023 (1999); Eur. Phys. J. C **20**, 313 (2001)
36. A. Capella, E.G. Ferreiro, A.B. Kaidalov, C.A. Salgado, Nucl. Phys. B **593**, 336 (2001); Phys. Rev. D **63**, 054010 (2001)
37. M.B. Gay Ducati, E.G. Ferreiro, M.V.T. Machado, C.A. Salgado, Eur. Phys. J. C **24**, 109 (2002)
38. A.M. Staśto, K. Golec-Biernat, J. Kwieciński, Phys. Rev. Lett. **86**, 596 (2001)
39. J. Bartels, K. Golec-Biernat, H. Kowalski, preprint DESY-02-037 (hep-ph/0203258)
40. E. Iancu, K. Itakura, L. McLerran, preprint SACLAY-T02/027 (hep-ph/0203137), to appear in Nucl. Phys. A; S. Munier, hep-ph/0205319
41. J. Bartels, K. Golec-Biernat, K. Peters, Eur. Phys. J. C **17**, 121 (2000)
42. C.W. De Jager, H. De Vries, C. De Vries, Atom. Data Nucl. Data Table **14**, 479 (1974)
43. E665 Collaboration, M.R. Adams et al., Z. Phys. C **67**, 403 (1995)
44. NMC Collaboration, M. Arneodo et al., Nucl. Phys. B **481**, 3 (1996)
45. NMC Collaboration, M. Arneodo et al., Nucl. Phys. B **481**, 23 (1996)
46. NMC Collaboration, P. Amaudruz et al., Nucl. Phys. B **441**, 3 (1995)
47. HERMES Collaboration, K. Ackerstaff et al., Phys. Lett. B **475**, 386 (2000)
48. X.-F. Guo, J.-W. Qiu, W. Zhu, Phys. Lett. B **523**, 88 (2001)
49. HERMES Collaboration, A. Bruell et al., in Proceedings of the X International Workshop on Deep Inelastic Scattering (DIS2002), Cracow, Poland, April 30–May 4, 2002
50. Z. Huang, H.J. Lu, I. Sarcevic, Nucl. Phys. A **637**, 79 (1998)
51. S.-Y. Li, X.-N. Wang, Phys. Lett. B **527**, 85 (2002)
52. A.H. Mueller, D.N. Triantafyllopoulos, preprint CU-TP-1057 (hep-ph/0205167)
53. M. Arneodo et al., in Proceedings of the Workshop on Future Physics at HERA (Hamburg, Germany, September 1995); H. Abramowicz et al., in TESLA Technical Design Report, Part VI, Chapter 2, edited by R. Klanner, U. Katz, M. Klein, A. Levy; EIC White Paper, preprint BNL-68933, edited by A. Deshpande, R. Milner, R. Venugopalan